Analysis of the first Feshbach resonances in electron collisions in rare gases

D. Dubé,* D. Tremblay, and D. Roy
Laboratoire de Physique Atomique et Moléculaire, Département de Physique, Université Laval, Cité Universitaire, Québec, Canada G1K 7P4
(Received 2 October 1992)

In this paper we present an analysis of the Feshbach resonances located below the first inelastic threshold in helium, neon, argon, krypton, and xenon. The measurements were made with an electron-scattering spectrometer called MAPDESS capable of simultaneous measurements at up to 19 angles, ranging from 18° to 162°. Data are analyzed using single-phase-shift formalism to evaluate the angle-dependent form factors of the resonances, describing the interference of the resonant amplitude with the nonresonant one. For each gas, the use of data at many angles enables a precise evaluation of the first three or four phase shifts and the resonance width. In some cases, the agreement of the analyzed experiment and theory is not perfect at small and large scattering angles.

PACS number(s): 34.80.Bm

INTRODUCTION

Since 1963, when Schulz [1] observed the *e*-He resonance near 19.36 eV, much experimental and theoretical work has been done on the study of electron-atom- and electron-molecule-scattering resonances. Descriptions of the first Feshbach resonances with classical scattering theory using Fano's approach have given very good results in past years. With this approach, the phase shifts at resonance energy and the natural width of resonance are the only data needed to describe the observed structure. Thus, by properly analyzing these phenomena, one can accurately deduce these quantities. Until now, the techniques that have been used to analyze resonances did not fully exploit the angular behavior of cross-section measurements. In this paper, we present an approach that enables one to deduce phase shifts from the angular dependence of resonance profile shape parameters and to obtain a precise value for the natural width using the relative strength of a resonance as a function of the scattering angle. This method is then applied to the study of the first Feshbach resonances in rare gases using data obtained with a multidetection electron spectrometer.

EXPERIMENT

The measurements of resonance profiles at various angles have been performed using a nonconventional electron-scattering spectrometer featuring multiangle parallel detection, the MAPDESS. This spectrometer has been fully described elsewhere [2] and we just briefly describe its main features. It is based on a truncated spherical mirror analyzer that can simultaneously select scattered electrons at 19 angles from 18° to 162° with an angular resolution of ±3°. A monochromatic beam of electrons is focused at the collision center near the exit of a hypodermic needle from which the target gas is introduced in the vacuum chamber. From this point, the scattered electrons reach the analyzer entrance and are analyzed. The present work represents the first systematic measurements that were made with this spectrometer. Some measurements (in argon) were made when only ten detectors were operational.

For measurements related to the first Feshbach resonance in a rare gas, the incident-electron energy does not allow inelastic collisions; thus the analyzer can be operated at poorer resolution in order to increase transmission. However, for measurements in helium, one can benefit from analyzer selection in reducing the thermal broadening effect at large angles [3]. The electrons are collected at the exit of the analyzer by 19 electron multipliers. Pulses are amplified, filtered, shaped, and then counted using a homemade data-acquisition system specially designed to handle parallel counting of events. This system sweeps primary electron energy while accumulating data. A custom highly interactive software which adds ease of use to performance has proved to be very helpful in spectrometer tuning and running.

Data presented in this work have been measured using an incident energy resolution in the range 30–50 meV. With this resolution, incident currents over 10 nA have been achieved. In these conditions, it was possible to obtain a very good signal-to-noise ratio at all scattering angles with runs of less than 24 h. In view of the method of analysis, this approach was preferred to the use of a higher resolution that would have cost an important decrease in signal intensity for which an increase in accumulation time could hardly compensate. The measurements as such are not presented in this work; however, the curves for the cases of helium and neon were shown in our previous work [2].

METHOD OF ANALYSIS

In the partial-wave formalism, the description of the differential cross section depends on whether or not spin effects have to be taken into account [4]. In both cases, it is possible to establish relations between general cross-section equations and a Fano profile expression, knowing that in the vicinity of the resonance one of the potential scattering phase shifts δ_l changes rapidly with energy E according to

$$\delta_L^r = \delta_L - \arctan\varepsilon^{-1} \tag{1}$$

with

$$\varepsilon = \frac{E - E_r}{\frac{1}{2}\Gamma} , \tag{2}$$

where E_r is the resonance energy, Γ is the natural width of the resonance, and $l = L$ corresponds to the partial wave in which the resonance occurs.

For spin-independent scattering, as in the case of helium, the cross section $\sigma(E,\theta)$ is given by Eqs. (3)–(5):

$$\sigma(E,\theta) = A^2 + B^2 , \tag{3}$$

$$A = \frac{1}{2K} \sum_{l=0}^{\infty} (2l+1)(\cos 2\delta_l - 1) P_l(\cos\theta) , \tag{4}$$

$$B = \frac{1}{2K} \sum_{l=0}^{\infty} (2l+1)(\sin 2\delta_l) P_l(\cos\theta) , \tag{5}$$

where K is the electron momentum and $P_l(\cos\theta)$ are the Legendre polynomials.

In introducing Eq. (1) in these expressions, one can obtain the Fano profile expression that we write using symmetric and antisymmetric terms [5,6]:

$$\sigma(\theta) = X \left[1 + \frac{Y}{\varepsilon^2+1} + \frac{Z\varepsilon}{\varepsilon^2+1} \right] , \tag{6}$$

where the parameters are given by

$$X = a^2 + b^2 + t^2 + 2t(a\cos 2\delta_L + b \sin 2\delta_L) , \tag{7}$$

$$Y = \frac{-4t(a\cos 2\delta_L + b\sin 2\delta_L)}{X} , \tag{8}$$

$$Z = \frac{4t(a\sin 2\delta_L - b\cos 2\delta_L)}{X} , \tag{9}$$

with

$$a = \frac{1}{2K} \sum_{l \neq L} (2l+1)(\cos 2\delta_l - 1) P_l(\cos\theta) - \frac{1}{2K}(2L+1) P_L(\cos\theta) , \tag{10}$$

$$b = \frac{1}{2K} \sum_{l \neq L} (2l+1)(\sin 2\delta_l) P_l(\cos\theta) , \tag{11}$$

and

$$t = \frac{1}{2K}(2L+1) P_L(\cos\theta) . \tag{12}$$

From these equations, one can see that if the values of X, Y, and Z are known from experimental data for many scattering angles, it is possible to deduce values of phase shifts that best describe these observations. Thus the first step of the analysis is to obtain precise values for the X, Y, and Z parameters from experimental resonance measurements at several angles. The same procedure is used to obtain similar equations in the case of spin-dependent scattering.

Of these three parameters X is the most difficult to measure since it represents the constant signal strength off resonance. The values of Y and Z can be obtained with precision from experimental data if one knows the exact value of the natural width of the resonance. Since this is not the case, we must choose a parameter that does not depend strongly on the natural width assumption to obtain the values of phase shifts. The shape factor q used in the well-known Fano expression exhibits this behavior. Its value can be obtained from experimentally fitted parameters Y and Z through

$$q = \frac{Y + (Y^2+Z^2)^{1/2}}{Z} . \tag{13}$$

The second step of the analysis consists of fitting the values of phase shifts to the experimental q obtained at various angles. Since we get up to 19 profile indexes, it is possible to fit the first three or four phase shifts. Higher partial waves are approximated by [7]

$$\delta_l = \arctan\left[\frac{\pi\alpha K^2}{(2l-1)(2l+1)(2l+3)} \right] , \tag{14}$$

where α is the dipole polarizability of the atom. The number of terms is chosen large enough so that with a larger number of terms the change of the phase shifts obtained is not significant. In general 11–15 terms were used.

At this point we get phase shifts that we use to compute theoretically predicted relative total amplitude (or strength) of resonance R. This factor represents the total amplitude of resonance divided by signal strength outside the resonance and is given by

$$R = (Y^2+Z^2)^{1/2} . \tag{15}$$

For the third and final step of the process, the measured amplitude is compared to the assumed amplitude and the natural width is corrected since an error in this value causes (with a good approximation) an inversely proportional error in the fitted amplitude.

Since this method relies on the accuracy of the initial Y and Z parameters, the experimental data must be analyzed by properly taking into account broadening effects. The broadening is mainly caused by the energy distribution of incident electrons and by the thermal velocity of target atoms (also known as Doppler broadening). Because of the high signal-to-noise ratio of our experimental data, the numerically simulated model must well describe the experimental conditions in order to achieve a good fit for each resonance. For this reason it is necessary to take into account the fact that the electron energy distribution is not quite symmetrical. This is simulated by using two half-Gaussian curves with slightly different widths. On the other hand, at the collision center, electrons are mainly scattered by the incoming gas from the needle. These atoms are preferentially oriented, thus reducing the effective velocity spread in the scattering plane. Since all atoms are not immediately pumped, a certain amount of gas stays in this area after the entrance in the vacuum. These atoms produce a second scattering source with a larger velocity spread. Those two sources have been taken into account in the fitting process.

The experimental data show that signal intensity

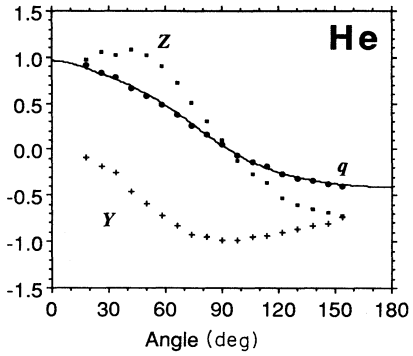

FIG. 1. Y, Z, and q parameters as a function of the scattering angle, deduced from data for helium ^2S resonance. The solid line is calculated with the phase shifts determined.

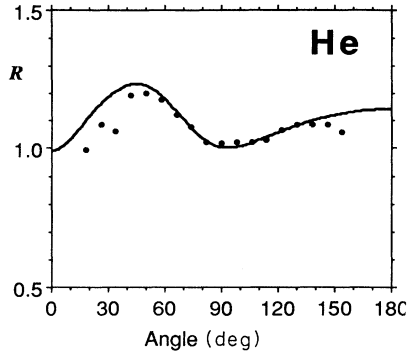

FIG. 2. Resonance relative amplitude as a function of the scattering angle, deduced from data for helium ^2S resonance. The solid line is calculated with the phase shifts determined.

changes with electron energy because of the physical process and of the evolution of the incident electron beam intensity with energy. This was simulated in the fitting process by adding a second-order polynomial to the profile. The energy position of each resonance has been obtained in the past and we did not try to determine it absolutely. The exact position of the resonance is fitted in the process in order to compensate correctly the error in the estimation of energy scale.

The numerical algorithm can be summarized in the following steps: (1) to evaluate the sum of Doppler-broadening Gaussians for incoming and diffuse gas; (2) to compute a theoretical Fano profile with trial X, Y, and Z values; (3) to evaluate the electron energy distribution; (4) to convolute the Fano profile, the Doppler-broadening distribution, and the electron energy distribution; (5) to compare the simulated profile with the measured one; (6) to correct parameters.

The process is repeated until a good fit is obtained according to the standard χ^2 test (χ^2 is defined as the sum, over the set of data, of the squares of the differences between the measured and the calculated data, relative to the latter). Technically, this simple procedure is more complicated because of the small natural width of the resonance. The experimental energy step between each data point is kept small (2.5 or 5 meV) in comparison to the width of the observed structure. But this energy interval is far too large to represent the neon ($\Gamma=1.3$ meV) profile properly, for example. For that reason we compute the theoretical curve using a variable energy interval between points. In the vicinity of the resonance, the frequency of computed points is increased to define the physical phenomenon correctly. Far from the resonance, the cross section varies slowly with energy and the theoretical curve is computed only in correspondence with the experimental points. When computing χ^2, only the points with correspondence in both sets of data are taken into account. Other aspects of the analysis procedure will be discussed in the last section.

HELIUM

Of all the first Feshbach resonances in rare gases, the helium $(1s2s^2)^2S$ resonance at 19.366 eV is the only one that has been measured with a resolution better than its natural width. Using electrons produced by photoionization as an electron source, Kennerly, Van Brunt, and Gallagher [8] measured the natural width of this reso-

TABLE I. Phase shifts of He at 19.37 eV (T: theoretical work; values in parentheses: estimated error on last figure).

	δ_0	δ_1	δ_2	
Nesbet (Ref. [9])	1.796	0.319	0.059	T
Golden *et al.* (Ref. [10])[a]	1.83(4)	0.354(12)	0.066(7)	
Kennerly *et al.* (Ref. [8])	1.813(17)	0.307(14)		
Williams (Ref. [11])[b]	1.794(25)	0.312(4)	0.058(5)	
Williams (Ref. [11])[c]	1.822(9)	0.310(5)	0.061(2)	
Williams and Willis (Ref. [12])	1.852(19)	0.309(8)	0.066(7)	
Andrick and Bitsch (Ref. [13])	1.81(9)	0.325(40)		
Cvejanović *et al.* (Ref. [14])	1.85(5)			
Gibson and Dolder (Ref. [15])	1.937	0.297	0.052	
Present work	1.778	0.317	0.076	

[a]Extrapolated using change rate obtained by Williams (Ref. [11]).
[b]Interpolated from Table I of Ref. [11].
[c]From resonance study.

nance and obtained 11.0±0.5 meV. We measured this resonance at the 19 angles and used the fitting algorithm to obtain Y and Z parameters assuming $\Gamma=10.5$ meV. At that stage, all the spectra were treated separately. The data from the 162° detector were not considered because of a large background signal. From that point, q and R values have been computed. Results are presented in Fig. 1. The third point (34°) exhibits a nonregular behavior. The corresponding detector is responsible since it caused a spurious background signal. The fit of the q values with phase shifts gives $\delta_0=1.778$, $\delta_1=0.317$, and $\delta_2=0.076$ and corresponds to the solid line in Fig. 1. These values are compared with previous works in Table I.

Using these phase shifts, the anticipated R values are computed. The results are shown in Fig. 2 with the experimental values. The fact that experimental R values are smaller than the anticipated ones indicates that the natural width had been overestimated. Using the R values obtained for the angles between 50° and 130°, we corrected the Γ value and obtained $\Gamma=10.3$ meV. The R values at low and large angles cannot be perfectly fitted by the used model. Increasing the apparent polarizability in the computations affects mainly low-angle resonances and could not explain the present results. In the analysis by Kennerly, Van Brunt, and Gallagher [8], the results obtained at 22° were not used to compute the phase shifts and the natural width. Using results at 90° and 135°, they concluded that the measure at 22° was in fact the behavior expected at 18°. The accuracy of our results will be discussed in the last section. Previous results are shown in Table II. This analysis of the helium resonance shows that the technique used to exploit multiangle data leads to consistent results.

TABLE II. Natural widths of the first Feshbach resonance of helium (T: theoretical work).

	Γ (meV)	
Burke *et al.* (Ref. [16])	11.72	T
Foster *et al.* (Ref. [17])	11.0	T
Hazi (Ref. [18])	11.5	T
Junker (Ref. [19])	11.72	T
Hata (Ref. [20])	34	T
Barden *et al.* (Ref. [21])	8.0	T
Berrington *et al.* (Ref. [22])	15.3	T
Bain *et al.* (Ref. [23])	12	T
Wickmann and Heiss (Ref. [24])	22	T
Sinfailam and Nesbet (Ref. [25])	15	T
Temkin *et al.* (Ref. [26])	14	T
Kennerly *et al.* (Ref. [8])	11.0±0.5	
Brunt *et al.* (Ref. [27])	9.0±1.0	
Roy *et al.* (Ref. [28])	8–10	
Cvejanović *et al.* (Ref. [14])	9±1	
Golden and Zecca (Ref. [29])	8±2	
Gibson and Dolder (Ref. [15])	8	
Andrick and Ehrhardt (Ref. [30])	15–20	
Simpson and Fano (Ref. [31])	10	
Present work	10.3	

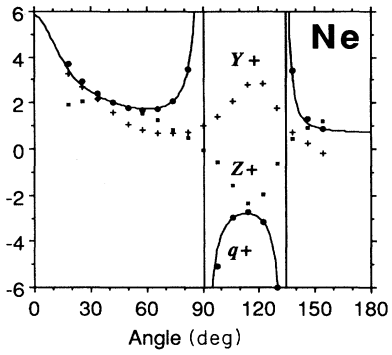

FIG. 3. $Y+$, $Z+$, and $q+$ parameters as a function of the scattering angle, deduced from data for neon $^2P_{3/2}$ resonance. The solid line is calculated with the phase shifts determined.

NEON

In the case of neon two resonances are observed [27], separated by only 97 meV, the first one being at 16.111 eV. These two profiles are fitted in the same computation to take correctly into account the overlap of the observed resonances. The first resonance corresponds to the formation of a $^2P_{3/2}$ ion state and is denoted by $+$, while the second corresponds to the formation of a $^2P_{1/2}$ state and is denoted by $-$. A natural width of 1.3 meV was assumed in the computations. The data obtained at 162° are rejected because of a large background signal.

The results of the fits are presented in Figs. 3 and 4. The profiles measured at 90° are very nearly symmetrical. In these conditions, absolute q values are very large and nonprecise. Thus we did not use those values in the phase-shift determination. Since the energy interval between the two resonances is very small, we kept the phase shifts constant for the two resonances. This enables us to fit the three first phase shifts with 34 q values. We get $\delta_0=-1.027$, $\delta_1=-0.349$, and $\delta_2=0.175$. As in the case of helium, δ_0 and δ_1 are in good agreement with values from other works but δ_2 is higher (see Table III for details). When the phase shifts are considered independent for the two types of coupling, but neglecting the

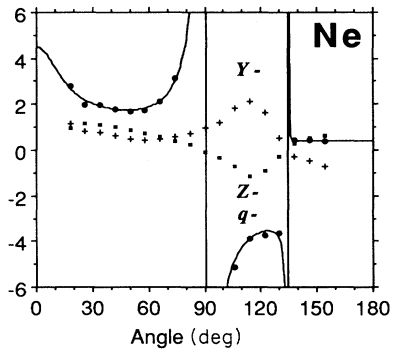

FIG. 4. $Y-$, $Z-$, and $q-$ parameters as a function of the scattering angle, deduced from data for neon $^2P_{1/2}$ resonance. The solid line is calculated with the phase shifts determined.

TABLE III. Phase shifts of Ne at 16.16 eV (T: theoretical work).

	δ_0	δ_1	δ_2	
Williams (Ref. [11])	−1.035(17)	−0.351(4)	0.150(5)	
Register and Trajmar (Ref. [32])	−1.031	−0.347	0.149	
Thompson (Ref. [33])	−1.036	−0.336	0.165	T
Peach (Ref. [34])	−1.033	−0.350	0.150	T
Dasgupta and Bhatia (Ref. [35])	−1.055	−0.363	0.139	T
Present work	−1.027	−0.349	0.175	

difference caused by the energy interval, we get $\delta_0=-1.032$, $\delta_1^+=-0.358$, $\delta_1^-=-0.348$, $\delta_2^+=0.175$, and $\delta_2^-=0.175$. Adding those two parameters gives an improvement of six units in χ^2 (from 37 to 31). For the p wave, the gap between δ_1^+ and δ_1^- is approximately five times larger than the difference caused by the energy change, assuming the change rate deduced from Williams's data [11]. This gap is greater for the p wave than for the d wave, as predicted theoretically by Fano and Rau [36].

The relative amplitude of the resonances is compared in Fig. 5 to the one obtained from the derived phase shifts. The two first angles were suffering from spurious signal (seen with no gas after the measurement and due to reflected electrons) and were not used in the Γ determination. It can be seen that the second resonance is nearly vanishing around 135°. Comparing measured to predicted amplitudes, we get no significant correction to the $\Gamma=1.30$ meV trial value. This value is compared with previous works in Table IV.

ARGON

The argon resonances are similar to the neon resonances. They are located [27] at 11.098 and 11.270 eV. In this case, the measurement has been performed with only ten detectors and the results of the fits are presented in Figs. 6 and 7 for the first and second resonances, respectively. The natural width is assumed to be 2.5 meV for the fits.

As in the case of neon, the energy interval between the two resonances is small and we suppose that the phase shifts are the same at the two energies. The values of q at 82° are not used because the resonances at this angle are very weak and the value of q changes rapidly at this angle. At 90° the observed profiles are nearly symmetrical as in neon and these data are not used in the phase-shift determination. As given in Table V, the results are $\delta_0=-1.220$, $\delta_1=-0.568$, $\delta_2=1.016$, and $\delta_3=0.122$. No significant difference is found between phase shifts for independent coupling.

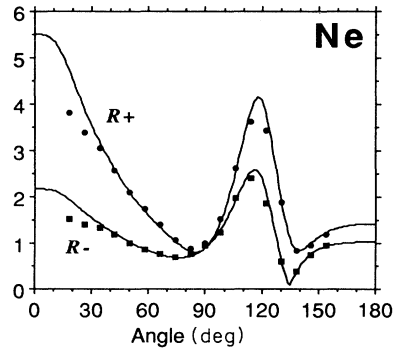

FIG. 5. Resonance relative amplitudes as a function of the scattering angle, deduced from data for neon $^2P_{3/2}$ and $^2P_{1/2}$ resonances. The solid line is calculated with the phase shifts determined.

The relative amplitude of the resonances is compared in Fig. 8 to the one obtained from the derived phase shifts. To correct the trial value of the natural width, the very low R value of the first resonance at 82° is not used. The 114° values are not used either since the R value is changing rapidly at this angle and the angular acceptance of the analyzer is not good enough to neglect neighbor contributions. Using all other data, one gets $\Gamma=2.3$ meV. This value is compared with previous works in Table VI. The value of Weingartshofer, Willmann, and Clarke [39] is estimated from a 90° symmetrical profile approximated by a triangular shape. This technique leads to systematic overestimation of $\pi/2$ for the natural width.

KRYPTON

The energy of the two first Feshbach resonances of krypton are 9.47 and 10.107 eV. The energy position of the second resonance is therefore higher than the first excitation level of the atom so that the negative temporary state formed in the resonance process can decay via this channel. This affects the observed profile [39]. We performed the measurement of the first resonance and assumed $\Gamma=4.0$ meV in the fits. The results are presented in Fig. 9. Three q values are rejected for the phase-shift determination: at 82° the observed resonance is too weak to be considered, at 74° the fits give nonrealistic electron source parameters, and at 122° the value of q is changing too rapidly. Using the 15 remaining q values, we get

TABLE IV. Natural widths of the first Feshbach resonances of neon.

	Γ (meV)
Brunt *et al.* (Ref. [27])	1.3±0.4
Roy *et al.* (Ref. [28])	1.4–1.8
Ehrhardt *et al.* (Ref. [37])	1.4
Simpson and Fano (Ref. [31])	>1
Present work	1.30

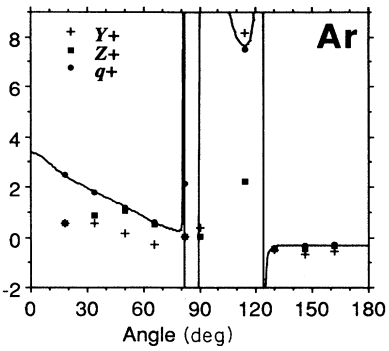

FIG. 6. $Y+$, $Z+$, and $q+$ parameters as a function of the scattering angle, deduced from data for argon $^2P_{3/2}$ resonance. The solid line is calculated with the phase shifts determined.

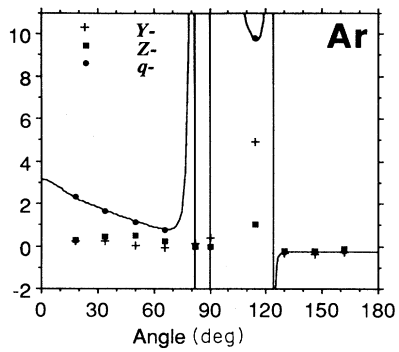

FIG. 7. $Y-$, $Z-$, and $q-$ parameters as a function of the scattering angle, deduced from data for argon $^2P_{1/2}$ resonance. The solid line is calculated with the phase shifts determined.

$\delta_0=-1.108$, $\delta_1=-0.603$, $\delta_2=1.072$, and $\delta_3=0.187$ (see Table VII). The δ_4 value is fixed at 0.0675 in the computations, as suggested by Fon, Berrington, and Hibbert [51].

Figure 10 shows the relative amplitude derived from the phase shifts compared with the measured one. To find the correction to the natural width, four values were eliminated. At 82° the resonance is too small, at 74° the fits give nonrealistic parameters, and at 114° and 122° the R value is changing too rapidly. Using all other data we obtained $\Gamma=3.6$ meV. This value is compared with previous works in Table VIII. The value determined by Weingartshofer, Willmann, and Clarke [39] is overestimated as in argon.

XENON

As in krypton, only the first Feshbach resonance of xenon is at an energy below the first excitation level. It is located at 7.77 eV, about 1.27 eV below the second one. The $^2P_{3/2}$ resonance has been measured and fitted using $\Gamma=4.5$ meV. Results are shown in Fig. 11. For the same reasons as in the other gases, data at 82°, 90°, 98°, and 122° are not used for the determination of the phase shifts. The results are $\delta_0=-1.14$, $\delta_1=-0.73$, $\delta_2=1.26$, and $\delta_3=0.26$ (see Table IX). The value of δ_4 is fixed at 0.077 from the works of McEachran and Stauffer [52] and Sin Fai Lam [50].

Figure 12 shows the relative amplitude derived from the phase shifts compared with the measured ones. The expected behavior is not confirmed by the experimental observation, especially at large angles. Using the data between 18° and 66°, we obtain $\Gamma=3.6$ meV, which is in fair agreement with the only available value of 4.5 meV (see Table X).

ERROR ESTIMATION

There are two main sources of error in the method used for data analysis. The first one arises from error in the expression for the differential cross section itself. The second one comes from error arising within the fitting al-

TABLE V. Phase shifts of Ar at 11.18 eV (T: theoretical work).

	δ_0	δ_1	δ_2	δ_3	
Srivastava *et al.* (Ref. [38])	−1.272	−0.448	0.991	0.178	
Williams (Ref. [11])	−1.173(21)	−0.587(16)	1.091(92)	0.107(25)	
Andrick and Bitsch (Ref. [13])	−1.224	−0.617	0.983	0.114	
Williams and Willis (Ref. [12])	−1.220(50)	−0.609(20)	1.092(20)	0.112(18)	
Weingartshofer *et al.* (Ref. [39])	−1.29	−0.61	1.17	0.10	
Thompson (Ref. [33])	−1.234	−0.605	1.086		T
Pindzola and Kelly (Ref. [40])	−1.409	−0.764	0.642	0.030	T
Yau *et al.* (Ref. [41])	−1.164	−0.523	1.486	0.144	T
Amusia *et al.* (Ref. [42])	−1.199	−0.585	0.943	0.129	T
O'Connell and Lane (Ref. [43])	−1.234	−0.600			T
Bell *et al.* (Ref. [44])	−1.260	−0.658	0.777	0.109	T
Dasgupta and Bhatia (Ref. [45])	−1.222	−0.595	0.876	0.115	T
Sienkiewicz and Baylis (Ref. [46])[a]	−1.245	−0.629	1.049	0.108	T
Sienkiewicz and Baylis (Ref. [46])[b]	−1.255	−0.626	1.058		T
Nahar and Wadehra (Ref. [47])	−1.351	−0.730	0.841	0.097	T
Present work	−1.220	−0.568	1.016	0.122	

[a]Relativistic treatment.
[b]Nonrelativistic treatment.

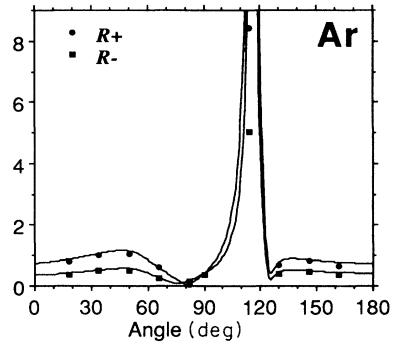

FIG. 8. Resonance relative amplitudes as a function of the scattering angle, deduced from data for argon $^2P_{3/2}$ and $^2P_{1/2}$ resonances. The solid line is calculated with the phase shifts determined.

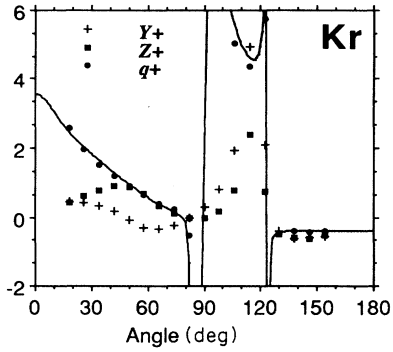

FIG. 9. $Y+$, $Z+$, and $q+$ parameters as a function of the scattering angle, deduced from data for krypton $^2P_{3/2}$ resonance. The solid line is calculated with the phase shifts determined.

gorithm as, for instance, an error coming from an improper modeling of the incident-electron beam or an inadequate ratio of contributions from the direct gas source and the diffuse source. We will first discuss the first one.

Actually, the expression used as a starting point to describe the measurements is not given exactly by Eq. (6) but by

$$I=a_0+a_1X\varepsilon+X\left[1+\frac{Y}{1+\varepsilon^2}+\frac{Z\varepsilon}{1+\varepsilon^2}\right] . \tag{16}$$

The term $a_1X\varepsilon$ was added to describe the variation with energy of the nonresonant cross section (in fact an $a_2X\varepsilon^2$ term was also considered but its effect is negligible for our purpose here). This variation comes from the energy dependence of the nonresonant scattering, and also from energy-varying electron optics properties. The constant a_0 describes an instrumental background contribution arising, for instance, from the dark count rate of the electron multiplier or from electrons detected but not originating from scattering events at the collision center. This term is assumed independent of energy. It is clear that a more meaningful description would be given by

$$I'=a_0'+X'(1+a_1'\varepsilon)\left[1+\frac{Y'}{1+\varepsilon^2}+\frac{Z'\varepsilon}{1+\varepsilon^2}\right] . \tag{17}$$

In this expression, the variation of X with energy is scaled directly by multiplication. Unfortunately, the fitting algorithm necessitates a great number of convolutions; it is thus much faster to deal with sum of terms as in Eq. (16) rather than a product as in Eq. (17).

One has to evaluate the error made on the evaluation of the X, Y, and Z by using Eq. (16) rather than (17).

TABLE VI. Natural widths of the first Feshbach resonances of argon.

	Γ (meV)
Brunt *et al.* (Ref. [27])	2.5±0.5
Weingartshofer *et al.* (Ref. [39])	3–4
Present work	2.3

Since these two equations are aimed at a description of the same experimental curve, we can equate Eqs. (16) and (17) to find the correspondence between the two descriptions. In the limit (to be justified below) where the slopes a_1 and a_1' are small, one finds

$$a_0'=a_0 \text{ (exact)} , \tag{18a}$$

$$X'\approx X(1-a_1Z) , \tag{18b}$$

$$Y'\approx Y+a_1Z(1+Y) , \tag{18c}$$

$$Z'\approx Z+a_1(Z^2-Y) , \tag{18d}$$

$$a_1'\approx a_1(1+a_1Z) . \tag{18e}$$

As an example, suppose that we have $a_1=0.001$. This means that the relative variation of the nonresonant cross section on a 1-eV energy interval is given by $a_1\Delta\varepsilon\approx 0.2$ in the case of helium with $\Gamma=10.3$ meV [following Eq. (2)], i.e., a variation of about 20% in this interval. This is significantly greater than the values normally encountered. Thus, as a rule, we can state that the measured variations on the nonresonant background with energy imply that a_1 is smaller than 0.001. This is still more true if the width Γ is smaller than for the helium case.

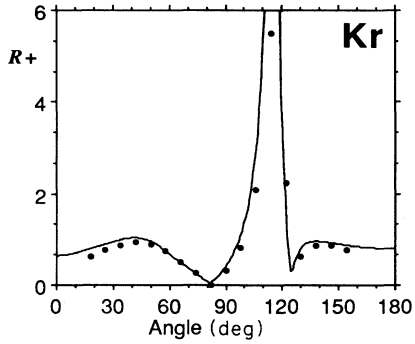

FIG. 10. Resonance relative amplitude as a function of the scattering angle, deduced from data for krypton $^2P_{3/2}$ resonance. The solid line is calculated with the phase shifts determined.

TABLE VII. Phase shifts of Kr at 9.47 eV (T: theoretical work).

	δ_0	δ_1	δ_2	δ_3	
Weingartshofer *et al.* (Ref. [39])	−0.91	−0.60	1.40	0.17	
Heindorff *et al.* (Ref. [48])[a]	−1.317	−0.734	0.980	0.142	
Srivastava *et al.* (Ref. [38])	−1.313	−0.591	0.947	0.230	
Yau *et al.* (Ref. [41])	−1.317	−0.611	1.339	0.213	T
Sin Fai Lam (Ref. [50])[b]	−1.254	−0.708	1.148	0.159	T
O'Connell and Lane (Ref. [43])	−1.242	−0.687	0.921		T
Fon *et al.* (Ref. [51])	−1.245	−0.732	0.961	0.130	T
McEachran and Stauffer (Ref. [52])	−1.240	−0.692	1.256	0.160	T
Present work	−1.108	−0.603	1.072	0.198	

[a]Deduced from Holtsmark (Ref. [49]).
[b]10 eV.

Then in most cases, a_1 is considerably smaller than 0.001.

If one defines q' as in Eq. (13) but with Y' and Z' replacing Y and Z, and in the same way one defines R'' from Eq. (15), Eqs. (18) yield

$$q' \approx q + a_1 \left[1 + \frac{qY}{Z} \right] \tag{19}$$

and

$$R' \approx R\,(1 + a_1 Z) \,. \tag{20}$$

This means that the more realistic q' and R' that one would get from Eq. (17) instead of (16) are close to the q and R values obtained from (16), taking into account the smallness of a_1. The consequence of all this is that the error made by using Eq. (16) instead of (17) is not significant in comparison with the other sources of errors.

Now, let us evaluate the effect of the instrumental background on the results. For simplicity, we set $a_1 = 0$; one can then rewrite Eq. (16) as

$$I'' = X'' \left[1 + \frac{Y''}{1+\varepsilon^2} + \frac{Z''\varepsilon}{1+\varepsilon^2} \right] , \tag{21}$$

with

$$X'' = X(1 + a_0/X) \,, \tag{22a}$$

$$Y'' = \frac{Y}{1 + a_0/X} \,, \tag{22b}$$

$$Z'' = \frac{Z}{1 + a_0/X} \,. \tag{22c}$$

Suppose that one erroneously assumes that a_0 is zero. The fitting algorithm will give values for X'', Y'', and Z'' instead of the real X, Y, and Z. Equations (22) tell that the apparent values of Y'' and Z'' are smaller than the real ones and that the apparent X'' is greater than the real X value. This has no consequence on the evaluation of the q value [see Eq. (13)] since it depends only on the Y/Z ratio, which is the same as Y''/Z''. On the contrary, the apparent relative intensities will then be [see Eq. (15)]

$$R'' = (Y''^2 + Z''^2)^{1/2} = \frac{(Y^2+Z^2)^{1/2}}{1 + a_0/X} = \frac{R}{1 + a_0/X} \,. \tag{23}$$

We have stated above that the value of q is not sensitive to a particular choice of Γ. Now we see that q is totally insensitive to an error in the evaluation of the background a_0. We can thus state with confidence that the variations of q with angles reported here can be trusted more than the Y and Z dependences, being much less sensitive to systematic errors (like erroneous assessments of Γ and a_0). Phase shifts deduced from q factors are thus thought to be very precise. Note that the precision on the exact values of X, Y, Z, and R is directly dependent on proper estimation of the instrumental background [Eq. (22)].

From results shown in Figs. 2 (He), 5 (Ne), 8 (Ar), 10 (Kr), and 12 (Xe), we see that measured R values are in general smaller at small and large angles than those expected from the phase-shift analysis. The contribution

TABLE VIII. Natural widths of the krypton $^2P_{3/2}$ first Feshbach resonance.

	Γ (meV)
Swanson *et al.* (Ref. [53])	3.8–6.0
Weingartshofer *et al.* (Ref. [39])	8
Present work	3.6

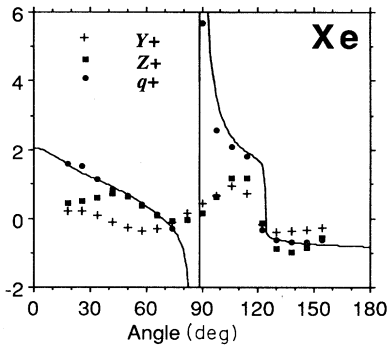

FIG. 11. $Y+$, $Z+$, and $q+$ parameters as a function of the scattering angle, deduced from data for xenon $^2P_{3/2}$ resonance. The solid line is calculated with the phase shifts determined.

TABLE IX. Phase shifts of Xe at 7.77 eV (T: theoretical work).

	δ_0	δ_1	δ_2	δ_3	
Heindorff *et al.* (Ref. [48])	−1.048(19)	−0.707(55)	1.306(11)	0.083(7)	
Yau *et al.* (Ref. [41])	−1.238	−0.661	1.632	0.353	T
Sin Fai Lam (Ref. [50])	−1.231	−0.722	1.221	0.232	T
O'Connell and Lane (Ref. [43])	−1.310	−0.743	0.169		T
McEachran and Stauffer (Ref. [52])	−1.318	−0.756	1.521	0.241	T
Czuchaj *et al.* (Ref. [54])	−1.292	−0.760	1.500	0.229	T
Present work	−1.14	−0.73	1.26	0.26	

from an instrumental background is at least partly responsible for that. Experience tells us that the background is greater at small and large angles. Is the background contribution large enough to account for the apparent discrepancy between the theoretical model and the measurements? The background intensity is very difficult to estimate. When the gas is cut off, the count rates at the detector become negligible, except sometimes at the smallest angles (18° and 26°) where one can detect a contribution coming directly from the incident-electron beam, in cases where the electron optics settings are inadequate. This is not the case at the other angles. The background contribution has a component proportional to pressure and this one is very difficult to estimate. This makes it difficult to decide whether or not this can explain the observed discrepancies found at small angles. Discrepancies observed at the largest angles can also be explained by some peculiar electron optics properties at the analyzer level observed at these angles. This point was discussed in detail in a previous work [55].

We now consider errors arising from the deconvolution process. In this study, the three steps of the analysis process generate errors. In the first step, experimental resonance measurements are fitted to obtain Y and Z values. Using the model described before, observed spectra are very well fitted and a reduced χ^2 approximately equal to 1 is achieved. Using a standard statistical criterion, the precision on Y and Z values is found to be better than 1% for almost all measurements. This error is higher on very weak resonances and corresponding data are eliminated in the next steps. On the other hand, the numerical errors were limited by using high-precision computation and increasing the density of simulated points around narrow shapes. Tests were conducted to assure that this type of error is not significant.

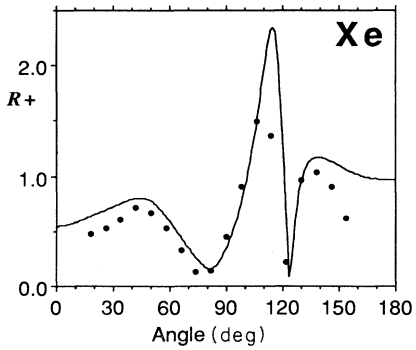

FIG. 12. Resonance relative amplitude as a function of the scattering angle, deduced from data for xenon $^2P_{3/2}$ resonance. The solid line is calculated with the phase shifts determined.

The last type of error arises from the imperfection of the model used to describe the conditions of the collision. For example, the energy distribution of the incoming electrons is described by an intuitive model using two half-Gaussians. To estimate roughly the error which could be induced by this approximation, we used a theoretical resonance profile ($\Gamma = 10$ meV) which we folded with a pure Gaussian distribution (width = 30 meV). We then fitted this profile with a parameter-adjusted resonance folded with a triangular distribution. In these conditions the Y and Z parameters are modified by 0–1 %. This value is a little larger for narrower resonances. The same results are obtained for nonsymmetric distributions. This situation is certainly worse than the representation actually used and consequently the error must be of the order of 1%. The experimental data do not allow an improvement in the simulation of the collision conditions since nearly all spectra were fitted up to the statistical limit. This cannot be achieved if one uses a symmetrical energy distribution for the electron beam or only one broadening source. We also checked that the ratio of the contributions from the direct gas beam to the diffuse (background) gas had only minor influence on the evolution of X, Z, and q, as far as realistic ratios are used.

Combining these errors we roughly estimate that the error on Y, Z, and R is of the order of 2% and of the order of 5% on q. Errors on phase shifts were not computed. Using these error estimations and adding the statistical fluctuations of the ratios of the expected R to the measured ones, we get an estimation of the accuracy of the natural widths. These values are summarized in Table XI.

CONCLUSION

It is known that the details of angular distributions are more difficult to calculate from a theoretical point of view since interference terms between partial waves have a de-

TABLE X. Natural widths of the xenon $^2P_{3/2}$ first Feshbach resonance.

	Γ (meV)
Heindorff *et al.* (Ref. [48])	4.5±1.0
Present work	3.6

TABLE XI. Summary of the natural widths of the first Feshbach resonances in rare gases with the estimated accuracy.

	Γ (meV)
Helium	10.3±0.3
Neon	1.30±0.15
Argon	2.3±0.2
Krypton	3.6±0.4
Xenon	3.6±1.0

cisive influence. Total cross section is less difficult since interference terms cancel out. However, the results reported here about the variation of the q shape factor with angles, especially when one compares results for neon, argon, krypton, and xenon, show systematic trends: near 90° and 125° the asymmetry factor varies very rapidly. On the other hand, one notes that the angular dependences of R, the relative strengths of the resonances, show in most cases discrepancies with theoretical curves at small and large angles. This could reveal that the theoretical model is not totally adequate. However, we can conclude that the agreement of the analyzed experiment and theory is not perfect at some angles, given the complexity of the data analysis and the fact that background contribution and electron optics characteristics certainly can partly account for this deviation at extreme angles.

ACKNOWLEDGMENTS

The authors are grateful to L. Dubé, A. Alikacem, and B. Tremblay for their collaboration and for fruitful discussions. This work has been supported by NSERC-Canada and Fonds FCAR du Québec. D.R. is a member of Centre de Recherches sur les Propriétés des Interfaces et la Catalyse (CERPIC) and the Network of Centers of Excellence on Molecular and Interfacial Dynamics (CEMAID/CEDMI).

*Permanent address: Département d'Informatique, Université du Québec à Hull, C.P. 1250, Succ. B, Hull, Québec, Canada J8X 3X7.

[1] G. J. Schulz, Phys. Rev. Lett. **10**, 104 (1963).
[2] D. Tremblay, D. Dubé, and D. Roy, Rev. Sci. Instrum. **60**, 879 (1989).
[3] F. H. Read, J. Phys. B **8**, 1034 (1974).
[4] N. F. Mott and H. S. Massey, *The Theory of Atomic Collisions,* 3rd ed. (Oxford University Press, London/New York, 1965).
[5] J. Corner and F. H. Read, J. Electron Spectrosc. **2**, 87 (1973).
[6] D. Andrick, in *Advances in Atomic and Molecular Physics,* edited by D. R. Bates and I. Estermann (Academic, New York, 1973), Vol. 9, p. 207.
[7] D. G. Thompson, Proc. R. Soc. London Ser. A **294**, 160 (1966).
[8] R. E. Kennerly, R. J. Van Brunt, and A. C. Gallagher, Phys. Rev. A **23**, 2430 (1981).
[9] R. K. Nesbet, J. Phys. B **12**, L243 (1979).
[10] D. E. Golden, J. Furst, and M. Mahgerefteh, Phys. Rev. A **30**, 1247 (1984).
[11] J. F. Williams, J. Phys. B **12**, 265 (1979).
[12] J. F. Williams and B. A. Willis, J. Phys. B **8**, 1641 (1975).
[13] D. Andrick and A. Bitsch, J. Phys. B **8**, 393 (1975).
[14] S. Cvejanović, J. Comer, and F. H. Read, J. Phys. B **7**, 468 (1974).
[15] J. R. Gibson and K. T. Dolder, J. Phys. B **2**, 741 (1969).
[16] P. G. Burke, L. C. G. Freitas, A. E. Kingston, and K. A. Berrington, in *Electronic and Atomic Collisions,* Abstracts of Contributed Papers, Thirteenth International Conference on the Physics of Electronic and Atomic Collisions, Berlin, 1983, edited by J. Eichler, W. Fritsch, I. V. Hertel, N. Stolterfoht, and U. Wille (ICPEAC, Berlin, 1983), p. 108.
[17] G. Foster, D. G. Hummer, and D. W. Norcross, Bull. Am. Phys. Soc. **24**, 1183 (1979).
[18] A. U. Hazi, J. Phys. B **11**, L259 (1978).
[19] B. R. Junker, Phys. Rev. A **18**, 2437 (1978).
[20] J. Hata, J. Chem. Phys. **66**, 1266 (1977).
[21] I. R. Barden, C. Bottcher, and K. R. Schneider, J. Phys. B **8**, L1 (1975).
[22] K. A. Berrington, P. G. Burke, and A. L. Sinfailam, J. Phys. B **8**, 1459 (1975).
[23] R. A. Bain, J. N. Bardsley, B. R. Junker, and C. V. Sukumar, J. Phys. B **7**, 2189 (1974).
[24] E. Wickmann and P. Heiss, J. Phys. B **7**, 1042 (1974).
[25] A. L. Sinfailam and R. K. Nesbet, Phys. Rev. A **6**, 2118 (1972).
[26] A. Temkin, A. K. Bhatia, and J. N. Bardsley, Phys. Rev. A **5**, 1663 (1972).
[27] J. N. H. Brunt, G. C. King, and F. H. Read, J. Phys. B **10**, 1289 (1977).
[28] D. Roy, A. Delâge, and J. D. Carette, J. Phys. E **8**, 109 (1975).
[29] D. E. Golden and E. Zecca, Rev. Sci. Instrum. **42**, 210 (1971).
[30] D. Andrick and H. Ehrhardt, Z. Phys. **192**, 99 (1966).
[31] J. A. Simpson and U. Fano, Phys. Rev. Lett. **11**, 158 (1963).
[32] D. F. Register and S. Trajmar, Phys. Rev. A **29**, 1785 (1984).
[33] D. G. Thompson, J. Phys. B **4**, 468 (1971).
[34] G. Peach, Comments At. Mol. Phys. **11**, 101 (1982).
[35] A. Dasgupta and A. K. Bhatia, Phys. Rev. A **30**, 1241 (1984).
[36] U. Fano and A. R. P. Rau, *Atomic Collisions and Spectra* (Academic, New York, 1986).
[37] H. Ehrhardt, L. Langhans, F. Linder, and H. S. Taylor, Phys. Rev. **173**, 222 (1968).
[38] S. K. Srivastava, H. Tanaka, A. Chutjian, and S. Trajmar, Phys. Rev. A **23**, 2156 (1981).
[39] A. Weingartshofer, K. Willmann, and E. M. Clarke, J. Phys. B **7**, 79 (1974).
[40] M. S. Pindzola and H. P. Kelly, Phys. Rev. A **9**, 323 (1974).
[41] A. W. Yau, R. P. McEachran, and A. D. Stauffer, J. Phys. B **13**, 377 (1980).
[42] M. Y. Amusia, N. A. Cherepkov, L. V. Chernysheva, D. M. Davidovic, and V. Radojevic, Phys. Rev. A **25**, 219 (1982).
[43] J. K. O'Connell and N. F. Lane, Phys. Rev. A **27**, 1893

(1983).
[44] K. L. Bell, N. S. Scott, and M. A. Lennon, J. Phys. B **17**, 4757 (1984).
[45] A. Dasgupta and A. K. Bhatia, Phys. Rev. A **32**, 3335 (1985).
[46] J. E. Sienkiewicz and W. E. Baylis, J. Phys. B **20**, 5145 (1987).
[47] S. N. Bahar and J. M. Wadehra, Phys. Rev. A **35**, 2051 (1987).
[48] T. Heindorff, J. Höfft, and P. Dabliewicz, J. Phys. B **9**, 89 (1976).
[49] J. Holtsmark, Z. Phys. **66**, 49 (1930).
[50] L. T. Sin Fai Lam, J. Phys. B **15**, 119 (1982).
[51] W. C. Fon, K. A. Berrington, and A. Hibbert, J. Phys. B **17**, 3279 (1984).
[52] R. P. McEachran and A. D. Stauffer, J. Phys. B **17**, 2507 (1984).
[53] N. Swanson, J. W. Cooper, and C. E. Kuyatt, Phys. Rev. A **8**, 1825 (1973).
[54] E. Czuchaj, J. Sienkiewick, and W. Milaszewski, Chem. Phys. **116**, 69 (1987).
[55] D. Tremblay and D. Roy, J. Phys. B **24**, 1867 (1991).